Journal of Fundamental and Applied Sciences

Research Article

ISSN 1112-9867

Available online at http://www.jfas.info

THEORETICAL STUDY OF THE REACTIVITY OF MONURON AND ITS PROTONATED FORMS

R. Masmoudi*, S. Khettaf, I. Boukhatem, R. Aberkane, C. Kahlat, A. Soltani, A. Dibi

Department of Chemistry, Faculty of Matter Sciences, University of Batna1, Algeria

Received: 13 August 2019 / Accepted: 21 March 2020 / Published online: 01 May 2020

ABSTRACT

A theoretical study of 3-(4-Chlorophenyl)-1,1-dimethylurea and its protonated isomers has been carried out, to emphasize the experimental results of the electrostatic interactions in the herbicide models, for investigating the implications taking place on the structural parameters starting from the gaseous phase to the aqueous one. It has been found that its functionalized structure gives us three protonated targets. The calculations has been performed on both neutral and protonated forms using Density Functional Theory (DFT) with the hybrid functional B3LYP. Many molecular parameters have been studied. To identify the reactive sites, our study has focused on the local and the global reactivity descriptors explaining the chemical reactivity. The calculations have demonstrated that the attacks on the aliphatic branched exocyclic positions are privileged to those of the aromatic ring. Studying the solvent effect has revealed that there is a change in the hierarchy of the electrophilicity. Various vibrational modes have been exploited to discuss the literary spectroscopic data.

Key words: DFT; Monuron; Proton affinity; Global and local reactivity descriptors; Solvation.

Author Correspondence, e-mail: redhachem@yahoo.fr

doi: http://dx.doi.org/10.4314/jfas.v12i2.3

1. INTRODUCTION

Pesticides are well known by their benefits in the agricultural field, but the exaggerated use of them has several damages on the soil and the aquatic ecosystems [1-9]. Among these chemicals, the Monuron ($C_9H_{11}ClN_2O$), (Figure 1), belongs to the phenyl-urea's class, which

is a kind of urea, in which one of the nitrogen's is substituted by a p-chlorophenyl group, while the other is substituted by two methyl groups. It plays the role of a xenobiotic herbicide. The Monuron molecule is considered as a nonselective herbicide that inhibits the photosynthesis. It was introduced in 1952, and has been used for controlling grasses and weeds, in the industrial sites and the drainage ditch banks[10]. It has been used at lower application rates, in the agricultural areas in some countries, as a post-emergence herbicide.

Besides its pollution effects, Monuron are classified as a persistent (The *half-life* of *Monuron*, in a soil field, ranges from less than 30 days to 166 days). In soil, Monuron is primarily biotransformed into metabolites. Monuron has a moderate mobility in most of soils [11-13]. Although the biodegradation process is slow, the degradation is most likely to occur in water. Monuron is not a volatile substance, and it is not affected by hydrolysis. However, a loss has been observed, due to the photolysis in the surface layers of water, only a small amount has been absorbed by its target, where the major part has entered the ground, water, or air [14]. For these agronomic and environmental aims, it is important to have information on this organic complex that takes place in the contact with the ground. As its action depends largely on the quantity of the moving water, and on the retention time in the soil; it is interesting to determine it in an aqueous solution. In the present work, diverse paths of Monuron protonation have been studied using Density Functional Theory (DFT). We have realized a geometrical optimization, a simulation of the attack on the exocyclic chain of Monuron different atoms, a determination of the reactive sites, an analysis and allocation of the normal modes of vibration, and the effect of solvation.

2. MATERIALS AND METHODS

The neutral and protonated Monuron study has undergone significant development for its applications in various chemical problems [15-18]. First, we've made a calculation of geometry optimization using DFT/6-311++G(d,p) chemistry model with the Gaussian16 software [19-22] without a specific parameterization of symmetry [23]. From the output file, the chemical properties, dipole moments as well as the frontier molecular orbitals HOMO and LUMO [23] have been consulted. The local minima has been verified by a frequency analysis of each optimized structure using the same model to obtain the zero point vibrational energy (ZPVE), reported and compared with the experimental literature values. No imaginary frequencies have been detected confirming that the stationary point corresponds to a minimum of the potential energy surface (PES). The global and the local reactivity parameters have been determined in order to characterize the reactive sites of the molecule. The IR

spectrum has allowed us to determine the preponderant absorption vibrational bands along with their frequencies. The shift between the theoretical and the experimental spectroscopic values is rationalized by a scale factor. The algorithm that deals with this kind of error is employed in Gaussian16. Consequently, to correct the vibrational anharmonicities, the vibrational frequencies have been scaled by a factor of 0.879 [24, 25]. All the geometries of the calculated electronic structures have been built and viewed using the graphical interface GaussView6.0. The effect of the solvent environment has been taken into account utilizing the CPCM solvation model [26, 27] with ε = 78.5 for water measured at 298.15 °K and 1 atm.

3. RESULTS AND DISCUSSION

A. Structure

The Monuron has been optimized using DFT/6-311++G(d,p) model chemistry within the gas phase. This last structure has been re-optimized without any symmetry constraints employing the CPCM model taking into account the effect of solvent environment. The optimized structure of Monuron is depicted in figure 1, the predicted geometrical parameters as well as the experimental data determined from RX experiment (values in parentheses) [28] are reported in table 1.

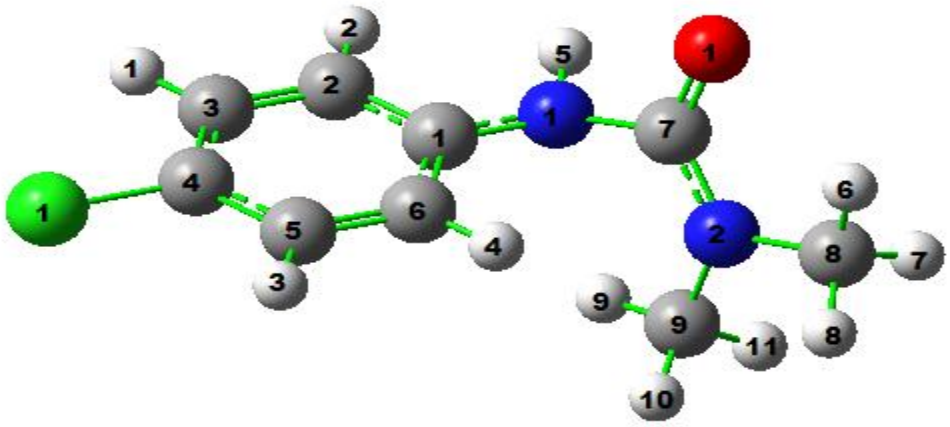

Fig.1. The optimized Structure of Monuron 3-(4-chlorophenyl)-1,1-dimethylurea

Table 1. Calculated and experimental structural parameters of Monuron

Bond distances (Å)		**Valence angles (°)**		**Dihedral angles (°)**	
C3 C2	1.39344 (1.39387)	C2 C3 C4	119.45827 119.28970	C4 C3 C2 C1	0.96892 (0.85940)
C3 C4	1.39527 (1.39523)	C3 C2 C1	120.95632 (120.83909)	C4 C3 C2 H2	-178.82919 (-179.10146)
C3 H1	1.08451 (1.08443)	C4 C3 H1	120.23602 (120.57035)	H1 C3 C2 C1	-179.73927 (-179.77749)
C2 C1	1.40491 (1.40519)	H1 C3 C2	120.30190 (120.13685)	H1 C3 C2 H2	0.46262 (0.26165)
C2 H2	1.08652 (1.08597)	C3 C2 H2	119.55104 (119.48836)	C2 C3 C4 C5	-0.69980 (-0.66842)
C1 C6	1.40313 (1.40339)	C1 C2 H2	119.49233 (119.67254)	C2 C3 C4 Cl1	179.38072 (179.45143)
C1 N1	1.41546 (1.41459)	C2 C1 C6	118.74870 (118.95513)	H1 C3 C4 C5	-179.99208 (179.97129)
C6 C5	1.39593 (1.39642)	C2 C1 N1	117.90135 (117.86947)	H1 C3 C4 Cl1	0.08843 (0.09115)
C6 H4	1.08385 (1.08382)	C6 C1 N1	123.33498 (123.15045)	C3 C2 C1 C6	-0.38275 (-0.24033)
C5 C4	1.39379 (1.39353)	C1 C6 C5	120.47707 (120.43275)	C3 C2 C1 N1	178.25685 (178.00075)
C5 H3	1.08464 (1.08449)	C1 C6 H4	120.03267 (120.35949)	H2 C2 C1 C6	179.41547 (179.72046)
C4 Cl1	1.74918 (1.76579)	C5 C6 H4	119.48638 (119.20492)	H2 C2 C1 N1	-1.94493 (-2.03846)
N1 C7	1.40608 (1.39955)	C4 C5 H3	120.08450 (120.46598)	N1 C1 C6 C5	-179.03883 (-178.72429)
C7 N2	1.37495 (1.36354)	C3 C4 C5	120.45264 (120.81688)	N1 C1 C6 H4	0.24064 (0.65709)
C7 O1	1.23052 (1.24241)	C3 C4 CL1	119.74149 (119.56420)	C2 C1 N1 H5	-41.26473 (-38.51949)
N2 C8	1.45974 (1.46120)	C5 C4 CL1	119.80582 (119.61881)	C2 C1 N1 C7	173.74430 (172.21862)
N2 C9	1.46073 (1.46324)	C1 N1 H5	114.03583 (114.54021)	C6 C1 N1 H5	137.30767 (139.64223)
C8 H6	1.08917 (1.08918)	C1 N1 C7	128.59380 (128.72379)	C6 C1 N1 C7	-7.68331 (-9.61966)
C8 H7	1.09884 (1.09779)	H5 N1 C7	109.02036 (110.49811)	C1 C6 C5 C4	0.74370 (0.77233)
C8 H8	1.09465 (1.09338)	N1 C7 N2	117.21465 (117.75378)	C1 C6 C5 H3	179.80994 (179.95942)
C9 H9	1.08803 (1.08823)	N1 C7 O1	119.66341 (119.34281)	C6 C5 C4 C3	-0.14922 (-0.14169)
C9 H10	1.09620 (1.09535)	N2 C7 O1	123.11077 (122.88704	C6 C5 C4 CL1	179.77021 (179.73839
C9 H11	1.09811 (1.09571)	C7 N2 C8	117.07443 (118.16351)	H3 C5 C4 C3	-179.21477 (-179.32386)
		C7 N2 C9	123.59934 (124.12397)	H3 C5 C4 CL1	0.70467 (0.55622
		C8 N2 C9	115.23026 (115.41920)	C1 N1 C7 N2	-46.69854 (-46.11152)

		H6 C8 H7	108.32926 (108.78517)	C1 N1 C7 O1	134.47904 (135.31756)
		H6 C8 H8	109.76020 (109.38753)	H5 N1 C7 N2	166.86207 (163.64890)
		H7 C8 H8	108.74540 (108.69728)	H5 N1 C7 O1	-11.96035 (-14.92202)
		N2 C9 H9	110.82591 (110.68803)	N1 C7 N2 C8	175.54137 (173.01193)
		N2 C9 H10	111.00407 (111.20751)	N1 C7 N2 C9	-28.34545 (-25.00787)
		N2 C9 H11	109.56785 (108.90047)	C7 N2 C9 H9	8.23565) (-0.95793)
				C7N2C9 H10	129.14985 (120.47484)
				C7N2C9 H11	-111.20330 (-119.97682)
				C8 N2 C9 H9	164.74614 (161.46720)
				C8 N2 C9 H10	-74.33965 (-77.10003)
				C8 N2 C9 H11	45.30719 (42.44831)
				C9N2C8 H6	170.62605 (165.54771)
				C9 N2 C8 H7	-69.45531 (-73.86144)
				C9 N2 C8 H8	50.54558 (45.88072)

The differences between the values are interpreted by very fact that the experimental data reported above were recorded in solid state, while the calculations are performed on an isolated molecule. within the solid state, the molecule adapts a conformation characterized by a torsion angle of -41.26° around the N1-C1binding, and the molecule isn't planar, this only can be accounted for an intermolecular hydrogen bonding [29]. The calculated values of dihedral angles (except for the latter case) reveals that the molecular structure features a planar conformation with a partial electron delocalization between the substituted phenyl group and the dimethyl-urea of the molecule: their values converge to180° or 0°, this former planar enforces the delocalization of electrons between these two systems. The benzene ring C=C bonds are equivalent at a length of 1.40 Å. The values of the N1 involving angles, C1N1C7, C6C1N1, C2C1N1 respectively 128.59°, 117.90, 123.33°close to 120°, as well as the Partial electron delocalization proves the Sp^2 nature of the atom. The analysis of both valence and torsion angles formed by N2 and the three surrounding atoms: C7, C8, C9 shows that the latter system features a triangular form. In addition to that, a remarkable

decrease in the length of both C=O bond (from 1.254 to 1.245 Å) and C1-N1 (from 1,411 to 1,326 Å) is also shown as a hybridization identity (Sp^2) for the atom N1 and N2. The similar behavior in the two atom systems, with a slight difference, is created by the rotation. With reference to the N1 atom, this rotation gives the impression that the molecule is separated into two parts: on one side, there's the phenyl, and on the other one, there's a relocation action resulting in. The angles bond lengths, obtained at the B3LYP/6-311G++(d,p) level, are in well agreement with the results obtained in the literature [28-36]. A frequency analysis of the optimized geometries verifies that the stationary points correspond to the minimum of the potential energy surface. In all cases, the frequencies values have been positive and no imaginary frequency has been obtained.

B. Charges and dipole moment

In order to locate the most likely protonation site(s) on the studied compound, an evaluation of the electron density on each atom of Monuron has been carried out. The obtained Mulliken charges are reported in table 2 (values in parentheses are for aqueous solution). Indeed, the determination of negative charge on each atom will help in the prediction of the most reactive sites toward the electrophilic medium.

Table 2. Values of the charges determined by DFT calculations

- **Neutral Monuron**

q_k(N)					
C1	-0.223 (-0.269)	C9	-0.383 (-0.381)	H4	0.165 (0.176)
C2	-0.844 (-0.763)	N1	-0.373 (-0.364)	H5	0.377 (0.388)
C3	-0.102 (-0.090)	N2	-0.229 (-0.207)	H6	0.191 (0.179)
C4	-0.179 (-0.209)	O1	-0.477 (-0.585)	H7	0.169 (0.180)
C5	-0.073 (-0.081)	Cl 1	0.222 (0.189)	H8	0.156 (0.173)
C6	0.576 (0.512)	H1	0.141 (0.157)	H9	0.169 (0.174)
C7	0.444 (0.495)	H2	0.123 (0.143)	H10	0.176 (0.188)
C8	-0.339 (-0.349)	H3	0.147 (0.166)	H11	0.165 (0.176)

- **charge (+1)**

q_k(N)					
C1	-0.533 (-0.516)	C9	-0.333(-0.359)	H4	0.163(0.182)
C2	-0.777 (-0.770)	N1	-0.217(-0.192)	H5	0.398(0.423)
C3	-0.068 (-0.014)	N2	-0.169(-0.116)	H6	0.202(0.186)
C4	-0.185 (-0.147)	O1	-0.343(-0.466)	H7	0.203(0.204)
C5	-0.043 (-0.075)	Cl 1	0.466(0.387)	H8	0.173(0.183)
C6	0.876 (0.833)	H1	0.189(0.191)	H9	0.160(0.174)
C7	0.423 (0.482)	H2	0.149(0.175)	H10	0.198(0.205)
C8	-0.325 (-0.362)	H3	0.197(0.202)	H11	0.194(0.190)

- **charge (-1)**

q_k(N)					
C1	0.324(-0.543)	C9	0.282 (-0.387)	H4	0.086 (0.153)
C2	-0.256(-0.257)	N1	-0.480(-0.462)	H5	0.377(0.373)
C3	-0.308(-0.538)	N2	-0.352(-0.166)	H6	0.129(0.176)
C4	0.107 (0.371)	O1	-0.531 (-0.625)	H7	-0.111(0.173)
C5	-0.372(-1.010)	Cl 1	0.096 (0.013)	H8	-0.335 (0.168)
C6	0.010 (0.597)	H1	0.073(0.106)	H9	0.002(0.171)
C7	0.280(0.472)	H2	-0.003 (0.106)	H10	-0.070 (0.183)
C8	0.415 (-0.336)	H3	-0.038(0.097)	H11	-0.324(0.166)

The positive charge on the hydrogen atom of the NH group indicates a high tendency to form a hydrogen bond with a high electronic density center. The negative charge on the nitrogen and oxygen atoms specifies their potentials for interacting with electrophilic species. For that reason, our interest is oriented towards studying these sites. From these results, it is obvious that the urea is the more reactive part of the molecule, assembling three different reactive sites. With regard to the dipole moment μ, the calculated values, in gaseous phase and aqueous phases, are respectively 2.51 and 3.54 Debye. The structural study has allowed us to show the geometric properties of Monuron and the assignment of protonation. The multi-basic structure reveals that the privileged protonation sites are three for Monuron. Therefore, three position isomers have been determined indicating the protonation on the exocyclic part of the molecule. The active sites of protonation O1, N1, and N2 are indicated by arrows for the examination of an electrophilic attack (figure 2).

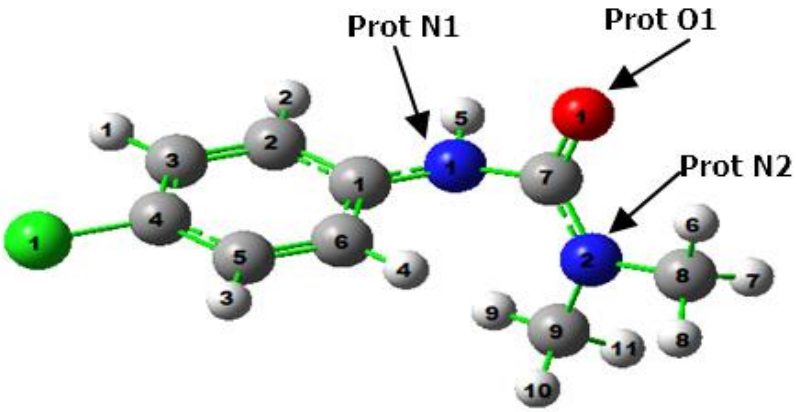

Fig.2. Structure of Monuron and active sites of protonation

According to table 3, it can be noticed that the geometry of the pesticide is almost not affected by protonation. Instead, it gives rise to hydrogen bond formation with O1, N1, and N2, respectively 0.967 Å and 1.016 Å.

Table 3. Calculated and experimental parameters of neutral and protonated Monuron

	Monuron			
		Protonated isomers		
	Neutral Monuron (X ray)	**N1**	**O1**	**N2**
C7 N1	1.3522	1.3341	1.39188	1.3516
N1 H9	2.9093	2.7117	2.5322	3.7270
N1 H9	2.9093	2.7117	2.5322	3.7270
O1 H8	3.5229	3.7008	3.9248	2.91616
O1 H10	3.7746	3.7008	4.2420	2.94916
O1 H			0.96721	
N2 H				1.01630
N1H		1.01630		
N2 C7 O1	122.357	130.96935	115.33184	97.6222
N2 C9 H9	109.464	109.65384	109.72670	109.69065
N1 H5 O1	25.194	44.1220	109.94873	63.8252
H N2 C8				109.75521
H N2 C9				172.23554
N1 H9 C9	70.121	108.78465	100.3730	71.4094
H O1 C7			-26.68481	
H N1 C6 C1		20.49327		
C2 C1 N1 H5	-47.342	-26.6848	4.9050	-4.7265

O1 C7 N2 C9	-159.795	0.22842	-92.30185	-56.4054
H5 O1 C7 N2	178.017	20.9359	131.1167	110.8396
N1 H9 C9 N2	-55.235p	6.4017	17.8924	55.2133
H N1 H5 O1		111.7740		
H N1 H9 C9		-8.54		
H N2 C8 H8				68.1678
H N2 C9 H10				-67.8027
H N2 C9 H10				-67.8027

H O1 C7 N1			69.5418	
H O1 C7 N2			-151.7409	

The calculations, made at the same level of theory, putting under consideration the effect of solvent environment has showed that this factor has no effect on the overall geometry of the studied molecules.

C. Energies and proton affinity

Initially, the energies have been determined in the gas phase for the neutral compound and for the three protonated forms, then, by introducing water as a solvent (values in parentheses), the effect of solvent has been taken into account by a single point calculation on optimized gas phase structure using the PCM (polarizable continuum Model)model [27]. The results are presented in table 4.

Table 4. Calculated energies at the B3LYP/6-311++G (d,p) level of theory in u.a

Calcul parameters : 6-31G++ (d.p)	E_T Monuron	E_T PROTN_1	E_T PROTO_1	E_T PROTN_2
(a.u)	-994.354240 (-994.365878)	-994.894124 (-994.906386)	-994.871247 (-994.879327)	-994.878521 (-994.891109)
(kcal/mol)	-623957.286 (-623964.5884)	-624296.063 (-624303.757)	-624281.707 (-624286.778)	-624286.272 (-624294.171)

The obtained results allow us to characterize the most potential protonation energetically preferred site. As we observe in the above results, the protonation path "PROT*N*1" of the

urea, in terms of energy, is the most suitable site for protonation. From a theoretical perspective, the Born-Oppenheimer approximation gives a lower energy than the real energy of the system, because of the relativistic consideration consisting that the nuclear movements are neglected. Therefore, a consideration of the zero point energy term must be taken into account. Thus, the proton affinity (PA) is corrected by the following relationship:

$$\mathbf{PA\ (M) = [E\ (M)\text{-}E\ (MH^{+})] + [ZPE\ (M)\text{-}ZPE\ (MH^{+})]}$$

Whereas (M) represents the neutral form, (MH^{+}) represents the protonated form.

Table 5. Proton affinity of neutral and protonated Monuron for 6-311G++ (d, p)

	ZPE (a.u)		**PA (Kcal/mol)**	
Monuron	0.190965	(0.190757)	**-**	**-**
ProtN_1	0.198545	(0.197209)	334.02076	(335.12014)
ProtO_1	0.199744	(0.199196)	318.91307	(316.893775)
ProtN_2	0.197990	(0.197288)	324.57814	(325.48425)

The obtained results in the table 5 shows that the protonation, at the level of the N1 atom, is more favorable than on O and N2 with an energy gap of 15.11 and 9.43Kcal/mol respectively by introducing the system energy absolute zero (ZPE). Taking into account the effect of solvent, the previous gap increases to 18.3 and 9.64 Kcal/mol. In the two conditions, the values' hierarchy of PA is respected in the protonated forms:

PA (prot (N1)) >PA (prot (O)) >PA (prot (N2))

D. Charges and dipole moment of protonated Monuron

The previously calculated values of point charges can be further exploited. For the explanation of the regioselectivity reaction, it can be done by the calculation of point charges, which has been performed to evaluate the electron density of the studied compound, and will let us confirm the sites of protonation for the studied compound. The results are shown in table 6.

Table 6. Values of the charges determined by DFT calculations

q_k(N)	**Monuron** **Neutral**	**Monuron protonated**		
		N_1	O_1	N_2
q H_5	0.377(0.388)	0.302 (0.334)	0.334 (0.363)	0.331 (0.360)
q N_1	-0.373(-0.364)	-0.487(-0.500)	-0.251(-0.290)	-0.173(-0.244)
q N_2	-0.229 (-0.207)	-0.162(-0.100)	-0.022(-0.207)	-0.358(-0.398)
q O_1	-0.477 (-0.585)	-0.452 (-0.457)	-0.460 (-0.445)	-0.359 (-0.416)
q C_7	0.444 (0.495)	0.301 (0.142)	-0.288 (-0.077)	0.238 (0.292)
q H		0.384 (0.348)	0.374 (0.400)	0.311 (0.316)

Mulliken charges on the three exo-cyclic sites of protonation, qualified protonation sites, comprised in the range of [-0.07, - 0.5] in aqueous medium. From these results, the protonation would occur preferentially at the level of part urea and more particularly on the N1 atom. As far as it concerns the dipole moment μ, the values calculated in gaseous phase and aqueous phase are presented in table 7.

Table 7. Values of the dipole moments

μ(Debye)	**Monuron**	**ProtN_1**	**ProtO_1**	**ProtN_2**
DFT / B3LYP6.31G++(d,p)	2.513012 (3.542955)	5.751480 (6.145991)	3.093578 (5.817873)	1.903265 (3.048268)

The obtained values show an increase in the dipole moment for the solvated form, which can be translated in a predisposition for binding to strongly polar site.

E. Frontier orbitals

The HOMO-LUMO energy gap, also known as hardness, is a significant indication of stability. Indeed, a large energy gap indicates a high stability of the molecule in a chemical reaction. In a comparison of the frontier orbitals energies of the three conjugate acid's isomers (table 8) shows that the energies of the occupied orbital frontier (HOMO) are respectively -0.206, -0.159, -0.215 and -0.216, -0.160, -0.232 in the gaseous and solvated phases leading to the conclusion that the protonated compounds are more stable than the neutral ones.

Table 8. Energies of frontier orbitals in u.a

	Monuron Neutre	**Monuron protonated**		
		ProtN_1	**ProtO_1**	**ProtN_2**
HOMO	-0.23146 (-0.22992)	-0.20616 (-0.21586)	-0.15966 (-0.16028)	-0.21552 (-0.23175)
LUMO	-0.03652 (-0.03281)	-0.02072 (-0.02640)	-0.02298 (-0.02592)	-0.04006 (-0.04585)
ΔE	0.19494 (0.19711)	0.18544 (0.18946)	0.13668 (0.13436)	0.17546 (0.1859)

In the following figures, we have depicted the graphical representation of the frontier molecular orbitals within the gaseous and aqueous phases.

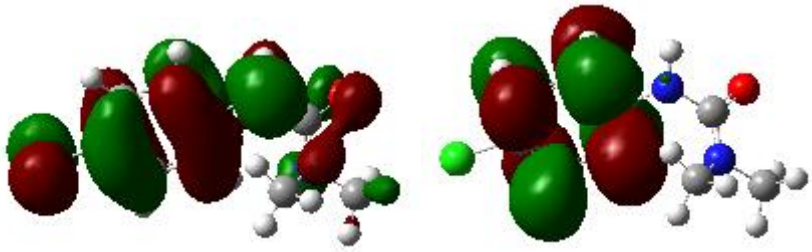

HOMO Isolated **LUMO Isolated**

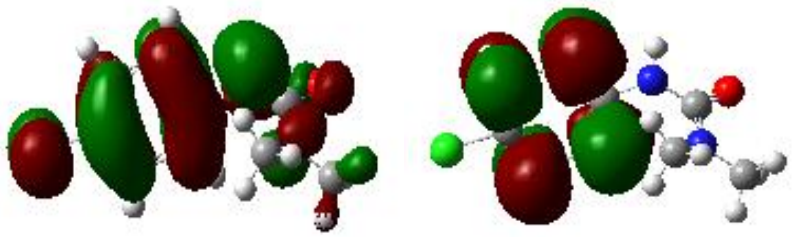

HOMO Solvated **LUMO Solvated**

Fig. 3. Schematic representation of the frontier orbitals for Monuron

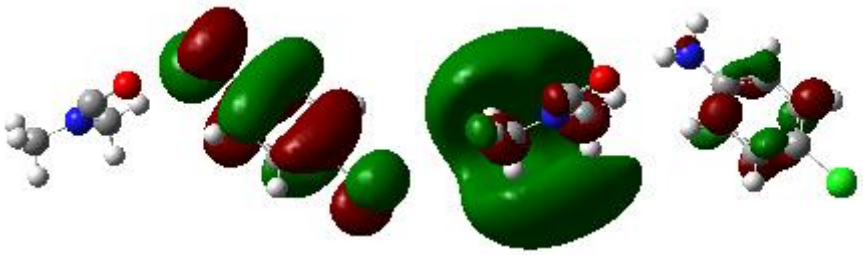

HOMO ProtN_1 isolated **LUMO ProtN_1 isolated**

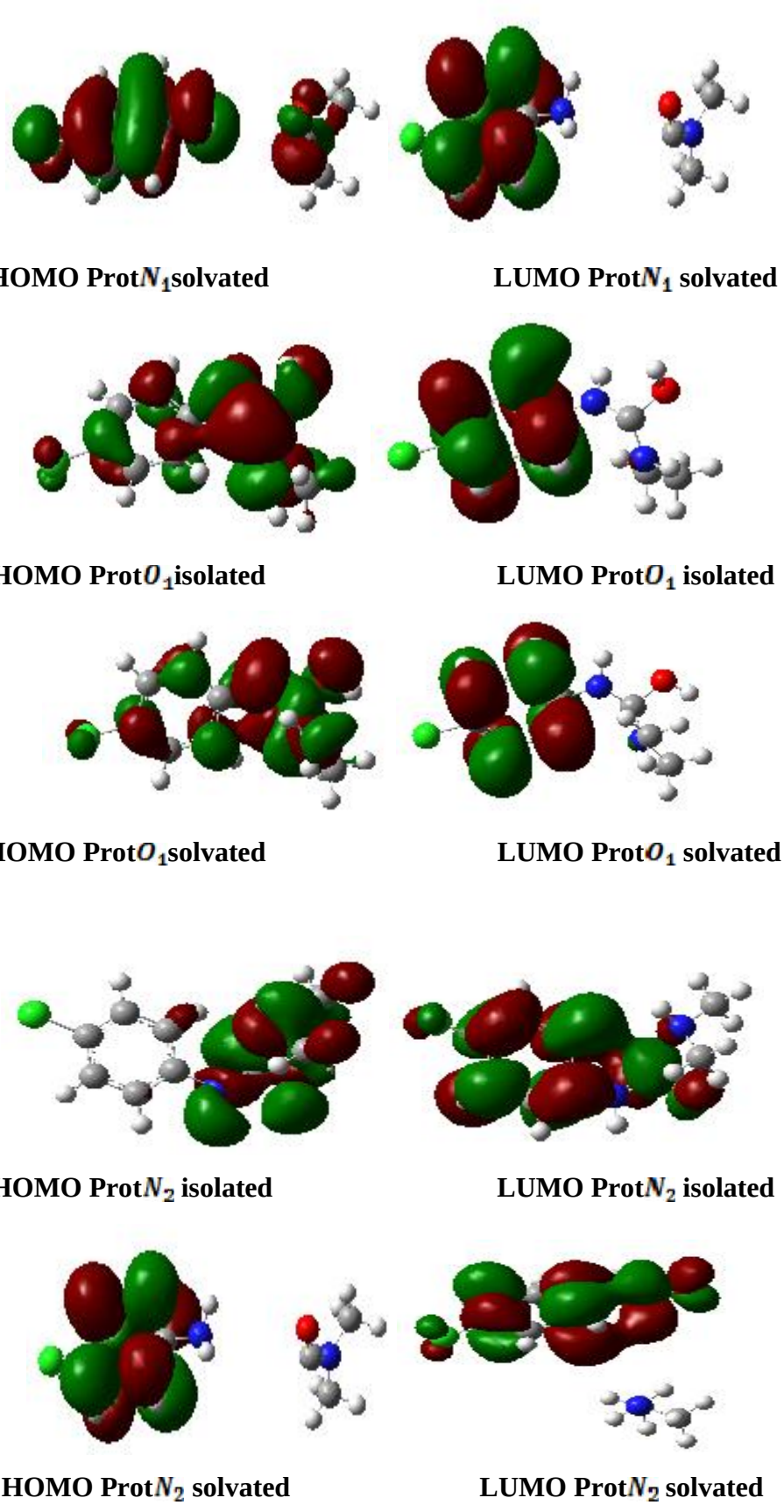

Fig.4. Schematic representation of the frontier orbitals for Protonated Monuron

The qualitative analyzing of the compounds HOMO orbitals shows that dimethyl-urea present a strong contribution among fragments, while the two LUMO orbitals are similar in the gas and aqueous phases. From a quantitative perspective, the difference in energy between the two frontier orbitals is less important in the protonated form of the pesticide; this means that the neutral form is more stable. A further analysis of the results shows that the solvation leads to similar results with a comparable increase in the gap between the frontier orbitals in the neutral and prot(N1) forms in the order of 0.3eV. The prot(O1) form has known a decrease of 0.2eV, which translates its relative instability. The obtained values emphasis the early ones as it concerns the Global indices reflecting the chemical reactivity of the studied systems.

F. Global and Local Reactivity Descriptors

In order to study the reactivity of Monuron, we focalize ourselves to the determination of global indices. Indeed, the global reactivity descriptors, derived from the conceptual Density Functional Theory, enable us to make connections with the general behavior of a molecule. The electronic affinity (EA) and the ionization potential (IP) are calculated with the two next formulas: EA = E(N-1) - E(N), IP = E(N) - E(N+1) where E(N) is the total ground state energy in the neutral, N electrons form, E(N-1) and E(N+1) represent the deficient (N-1) and exceeded (N+1) electron configurations, respectively. The parameters are the electronic chemical potential (μ), the electronegativity (χ), hardness (η) and the global electrophilicity index (ω), which can be determined using the following equations [37-42]:

$$\mu = -1/2\,(IP - EA)$$

$$\chi = -\mu$$

$$\eta = (IP - EA)$$

$$\omega = \frac{\mu^2}{2\eta}$$

Each of these parameters has its own meaning, for example, the electronic chemical potential can be translated to the escaping tendency of an electron [15]. The hardness η is directly proportional to the polarizability of the system [43,44]. The global electrophilicity index ω is an essential identifier of the molecule class; high and low values illustrate respectively the presence of good electrophiles and nucleophiles [44]. The obtained results are inserted in the table 10. The global reactivity descriptors in the aqueous phase has been similarly obtained at the B3LYP/6-311++G(d,p) level of theory.

Table 9. Global reactivity descriptors of Monuron at the B3LYP/6-311G++(d,p) level of theory in the gas phase and aqueous phase.

	E neutral	EN-1	EN+1	IP	EA	u	ή	ω_0	S	Nu
Gas phase	-27057,77	-27050,1667	-27057,6009	-0,16906438	7,60327308	3,88616873	-3,88616873	-1,94308436	-0,12866142	0,16906438
Aqueous phase	-27058,0867	-27052,2825	-27059,5678	1,4811165	5,8041642	2,16152385	-2,16152385	-1,08076193	-0,23131829	-1,4811165

The obtained results are in good agreement with the literature [45]. However, the latter parameters are global and do not show the distribution of the chemical reactivity on each specific site, it is primordial then, to move on to more detailed descriptors of local reactivity, this can be functionalized with Fukui indices, which exploit the electron density of each atom of the molecular system in different states (neutral, cation and anion) to calculate the Fukui indices, referred by f_k^+, f_k^-, f_k^0, allowing the most favorable sites to accept or lose the electronic density. In a molecule with N electrons, the Fukui functions for electrophilic, nucleophilic and free radical were proposed by Yang and Mortier [46] and has been expressed mathematically through the following equations:

$$f_k^+ = [q_k(N+1) - q_k(N)].$$

$$f_k^- = [q_k(N) - q_k(N-1)].$$

$$f_k^0 = \frac{1}{2}[q_k(N-1) - q_k(N+1)].$$

Whereas $q_k(N)$, $q_k(N+1)$,$q_k(N-1)$ are respectively the charge distribution of the atom k in the neutral, anionic and cationic molecule. Larger values of Fukui indices mean responsiveness of the site toward symmetry controlled reactions [47]. It is essential to reveal that the Fukui function values, obtained from various population schemes, may provide negative values. The determination of the various parameters, in the two phases, has led us to the values in the following tables and figure 4.

Table 10. Local reactivity descriptors of Monuron at the B3LYP/6-311G++ (d,p) level of theory in the gas phase.

atomes	q(N)	q(N+1)	q(N-1)	f_k^-	f_k^+	f°	ω_k+	ω_k-	N_k+	N_k-	S_k+	S_k-
C1	-0,269	-0,543	-0,516	0,247	-0,274	0,0135	0,29612877	-0,2669482	0,40582592	-0,3658357	0,06338121	-0,05713562
C2	-0,763	-0,257	-0,77	0,007	0,506	-0,2565	-0,5468655	-0,0075653	-0,7494449	-0,0103678	-0,11704705	-0,00161923
C3	-0,09	-0,538	-0,014	-0,076	-0,448	0,262	0,48418134	0,08213791	0,66354019	0,11256485	0,10363059	0,01758019
C4	-0,209	0,371	-0,147	-0,062	0,58	-0,259	-0,62684192	0,06700724	-0,85904757	0,09182922	-0,13416461	0,01434173
C5	-0,081	-1,01	-0,075	-0,006	-0,929	0,4675	1,00402783	0,00648457	1,37595723	0,0088867	0,21489469	0,00138791
C6	0,512	0,597	0,833	-0,321	0,085	0,118	-0,0918647	0,34692458	-0,1258949	0,4754384	-0,01966205	0,07425317
C7	0,495	0,472	0,482	0,013	-0,023	0,005	0,02485752	-0,0140499	0,03406568	-0,0192545	0,00532032	-0,00300714
C8	-0,349	-0,336	-0,362	0,013	0,013	-0,013	-0,0140499	-0,0140499	-0,0192545	-0,0192545	-0,00300714	-0,00300714
C9	-0,381	-0,387	-0,359	-0,022	-0,006	0,014	0,00648457	0,02377676	0,0088867	0,03258456	0,00138791	0,005089
N1	-0,364	-0,462	-0,192	-0,172	-0,098	0,135	0,10591467	0,18589105	0,14514942	0,25475204	0,02266919	0,03978675
N2	-0,207	-0,166	-0,116	-0,091	0,041	0,025	-0,0443112	0,09834934	-0,0607257	0,1347816	-0,00948405	0,02104996
O1	-0,585	-0,625	-0,466	-0,119	-0,04	0,0795	0,04323048	0,12861067	0,05924466	0,17625286	0,00925273	0,02752688
Cl 1	0,189	0,013	0,387	-0,198	-0,176	0,187	0,1902141	0,21399086	0,2606765	0,29326107	0,04071202	0,04580102
H1	0,157	0,106	0,191	-0,034	-0,051	0,0425	0,05511886	0,03674591	0,07553694	0,05035796	0,01179723	0,00786482
H2	0,143	0,106	0,175	-0,032	-0,037	0,0345	0,03998819	0,03458438	0,05480131	0,04739573	0,00855878	0,00740219
H3	0,166	0,097	0,202	-0,036	-0,069	0,0525	0,07457257	0,03890743	0,10219704	0,05332019	0,01596096	0,00832746
H4	0,176	0,153	0,182	-0,006	-0,023	0,0145	0,02485752	0,00648457	0,03406568	0,0088867	0,00532032	0,00138791
H5	0,388	0,373	0,423	-0,035	-0,015	0,025	0,01621143	0,03782667	0,02221675	0,05183908	0,00346977	0,00809614
H6	0,179	0,176	0,186	-0,007	-0,003	0,005	0,00324229	0,00756533	0,00444335	0,01036782	0,00069395	0,00161923
H7	0,18	0,173	0,204	-0,024	-0,007	0,0155	0,00756533	0,02593829	0,01036782	0,0355468	0,00161923	0,00555164
H8	0,173	0,168	0,183	-0,01	-0,005	0,0075	0,00540381	0,01080762	0,00740558	0,01481117	0,00115659	0,00231318
H9	0,174	0,171	0,174	0	-0,003	0,0015	0,00324229	0	0,00444335	0	0,00069395	0
H10	0,188	0,183	0,205	-0,017	-0,005	0,011	0,00540381	0,01837295	0,00740558	0,02517898	0,00115659	0,00393241
H11	0,176	0,166	0,19	-0,014	-0,01	0,012	0,01080762	0,01513067	0,01481117	0,02073563	0,00231318	0,00323846

The values of ω_k- obtained for N1, N2 and O1 are respectively0,185, 0,098 and 0,128 confirming that the most favorable site for an electrophilic attack is the N1 holding the Chloro-phenyl group. In regards to nucleophilic attack, it seems that the most qualified sites are C5 and C3 by 1.00, 0.48 respectively for ω_k+. The same approach was conducted for the study in an aqueous medium. The results are gathered in table 11.

Table 11. Local reactivity descriptors of Monuron at the B3LYP/6-311G++(d,p) level of theory in the aqueous phase.

atomes	q(N)	q(N+1)	q(N-1)	F_k-=q(N)-q(N-1)	F_k+=q(N+1)-q(N)	f°	ω_k+	ω_k-	N_k+	N_k-	S_k+	S_k-
C1	-0,223	0,324	-0,533	0,31	0,547	-0,4285	-1,06286714	-0,60235615	0,09247822	0,05240996	-0,0703778	-0,03988504
C2	-0,844	-0,256	-0,777	-0,067	0,588	-0,2605	-1,1425336	0,13018665	0,09940986	-0,01132731	-0,07565291	0,00862032
C3	-0,102	-0,308	-0,068	-0,034	-0,206	0,12	0,40027538	0,06606487	-0,03482726	-0,00574819	0,02650425	0,00437449
C4	-0,179	0,107	-0,185	0,006	0,286	-0,146	-0,5557221	-0,01165851	0,04835241	0,00101439	-0,03679717	-0,00077197
C5	-0,073	-0,372	-0,043	-0,03	-0,299	0,1645	0,58098222	0,05829253	-0,0505502	-0,00507193	0,03846976	0,00385984
C6	0,576	0,01	0,876	-0,3	-0,566	0,433	1,09978575	0,58292531	-0,0956904	-0,05071931	0,07282236	0,03859843
C7	0,444	0,28	0,423	0,021	-0,164	0,0715	0,31866584	-0,04080477	-0,02772656	0,00355035	0,02110047	-0,00270189
C8	-0,339	0,415	-0,325	-0,014	0,754	-0,37	-1,4650856	0,02720318	0,12747454	-0,0023669	-0,0970107	0,00180126
C9	-0,383	0,282	-0,333	-0,05	0,665	-0,3075	-1,2921511	0,09715422	0,11242781	-0,00845322	-0,0855598	0,00643307
N1	-0,373	-0,48	-0,217	-0,156	-0,107	0,1315	0,20791003	0,30312116	-0,01808989	-0,02637404	0,01376677	0,02007118
N2	-0,229	-0,352	-0,169	-0,06	-0,123	0,0915	0,23899938	0,11658506	-0,0207949	-0,01014386	0,01582535	0,00771969

O1	-0,477	-0,531	-0,343	-0,134	-0,054	0,094	0,10492656	0,2603733	-0,00912948	-0,02265463	0,00694772	0,01724063
Cl 1	0,222	0,096	0,466	-0,244	-0,126	0,185	0,24482863	0,47411258	-0,0213021	-0,04125171	0,01621134	0,03139339
H1	0,141	0,073	0,189	-0,048	-0,068	0,058	0,13212974	0,09326805	-0,0114964	-0,00811509	0,00874898	0,00617575
H2	0,123	-0,003	0,149	-0,026	-0,126	0,076	0,24482863	0,05052019	-0,0213021	-0,00439567	0,01621134	0,0033452
H3	0,147	-0,038	0,197	-0,05	-0,185	0,1175	0,35947061	0,09715422	-0,0312769	-0,00845322	0,02380236	0,00643307
H4	0,165	0,086	0,163	0,002	-0,079	0,0385	0,15350366	-0,00388617	-0,0133561	0,00033813	0,01016425	-0,00025732
H5	0,377	0,377	0,398	-0,021	0	0,0105	0	0,04080477	0	-0,00355035	0	0,00270189
H6	0,191	0,129	0,202	-0,011	-0,062	0,0365	0,12047123	0,02137393	-0,010482	-0,00185971	0,00797701	0,00141528
H7	0,169	-0,111	0,203	-0,034	-0,28	0,157	0,54406362	0,06606487	-0,0473380	-0,00574819	0,0360252	0,00437449
H8	0,156	-0,335	0,173	-0,017	-0,491	0,254	0,95405442	0,03303243	-0,0830106	-0,00287409	0,06317276	0,00218724
H9	0,169	0,002	0,16	0,009	-0,167	0,079	0,32449509	-0,01748776	-0,0282338	0,00152158	0,02148646	-0,00115795
H10	0,176	-0,07	0,198	-0,022	-0,246	0,134	0,47799875	0,04274786	-0,0415898	-0,00371942	0,03165071	0,00283055
H11	0,165	-0,324	0,194	-0,029	-0,489	0,259	0,95016825	0,05634945	-0,0826725	-0,00490287	0,06291543	0,00373118

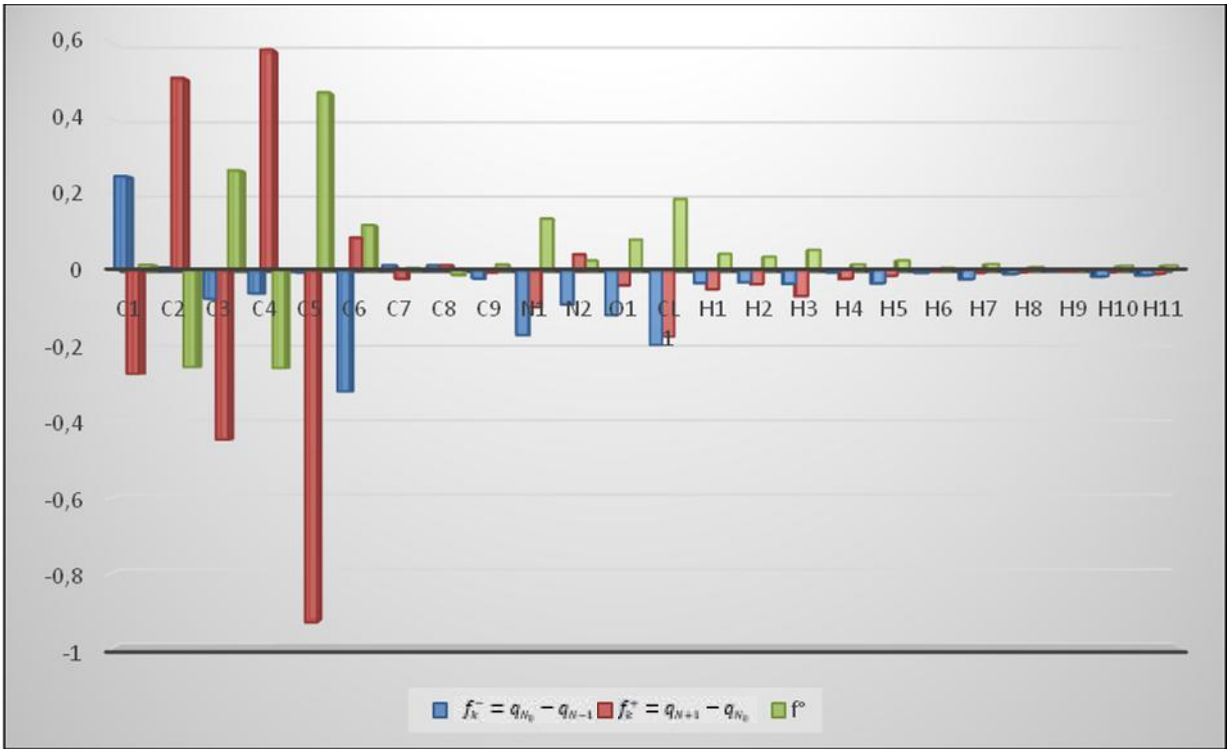

Fig.5. Fukui functions /aqueous phase.

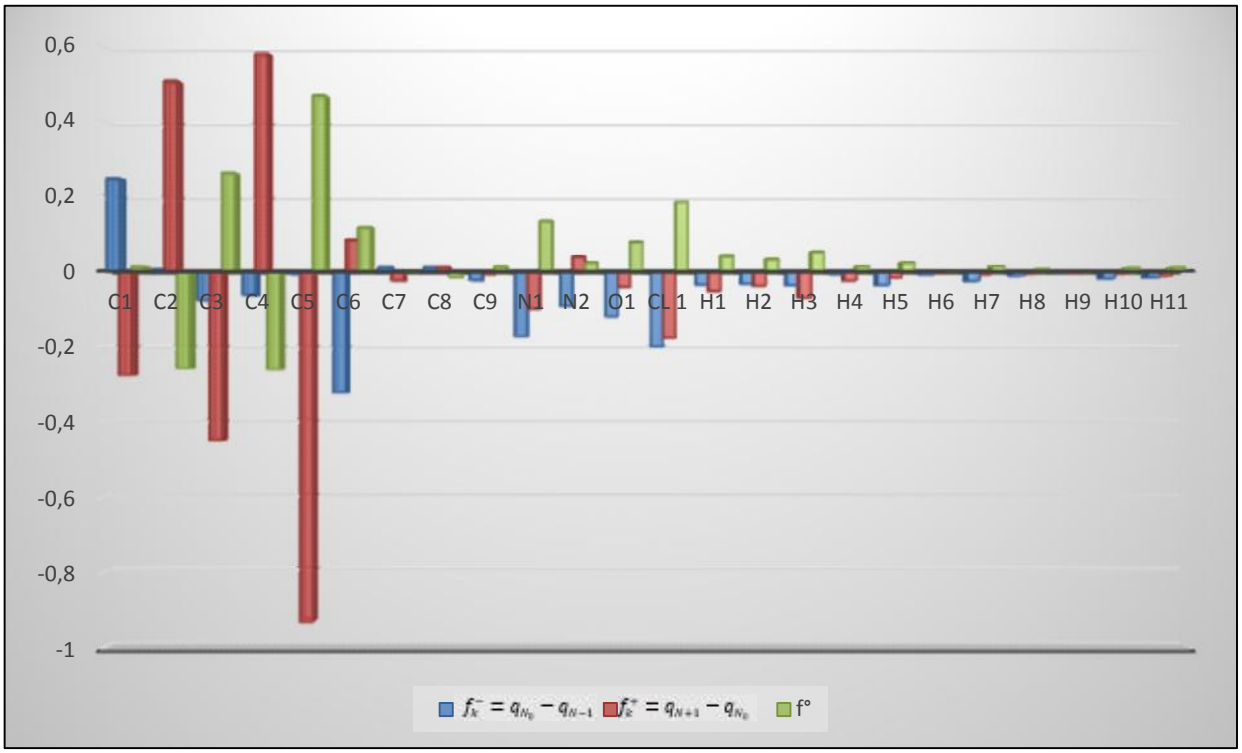

Fig.6. Fukui functions /Gas phase

The solvation leads to the same conclusion that an electrophilic attack will be the subject of the nitrogen N1 part of the urea on Monuron, however a nucleophilic attack is now targeting another electrophilic site on the molecule which is carbon labelled C6 with ω_k^+ of 1.1, that is the hierarchy of electrophilicity is changed to: N_k^+ (C8) = 0.1274 > N_k^+ (C9) = 0.1124

G. IR Study

In order to accomplish a spectroscopic comparative study, a frequency analysis was applied to each of the optimized structures of the neutral, protonated forms of the in both gaseous and aqueous phases (values in parenthesis), to verify that the stationary points correspond to the minimum of the potential energy surface. In all cases, the frequency values were positive and no imaginary frequency was obtained. Thus, the following preponderant vibrational frequencies were located: strong stretching vibrations of the carbonyl bond at 1701cm^{-1} (1648cm^{-1}), stretching N-H vibrations at 3578cm^{-1}(3564cm^{-1}) while N-C-N symmetric stretching vibrations were observed at 1021cm^{-1}(1023cm^{-1}).For phenyl-urea compounds, the results are in agreement with those obtained in the literature[48].

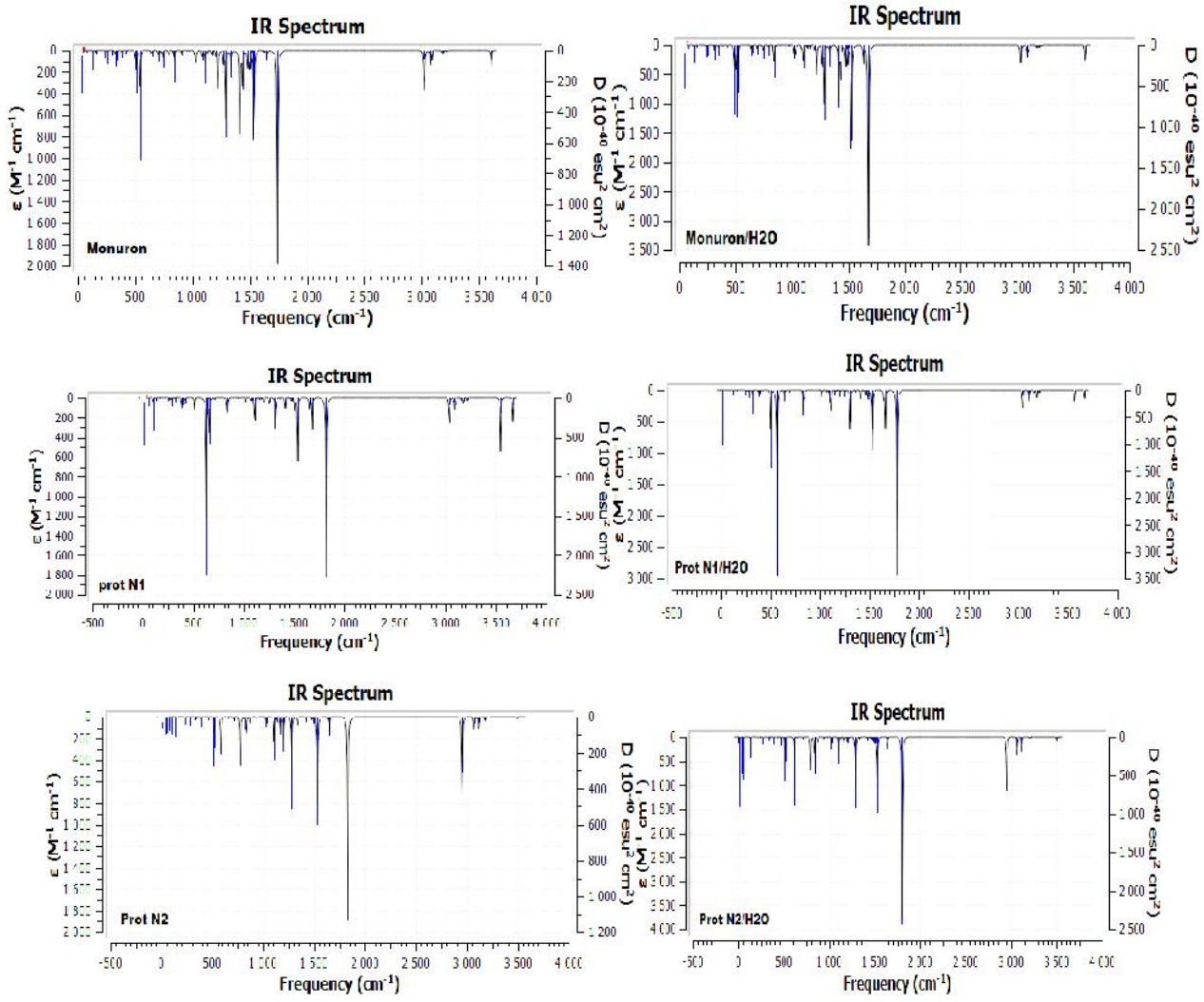

Fig.7. IR spectra of the neutral and protonated isomers of Monuron in gaseous and aqueous phases

The spectroscopic study of Monuron shows us the absorption bands in gaseous and aqueous phases: 437cm^{-1} (432cm^{-1}) band is characterizing the absorption of benzene ring cycle; 1599cm^{-1}

(1595cm^{-1}) correspond to the absorption of the C=C bonds for different isomers, 3100cm^{-1} and 3057cm^{-1} (3104cm^{-1} and 3068cm^{-1}) determine the absorption of the C-H for the two methyl groups; 3578cm^{-1} (3564cm^{-1}) and 1701cm^{-1} (1648 cm^{-1}) correspond to the absorptions of the N-H and the C=O bonds respectively. It may be noted that the appearance of the absorption bands with the frequencies 3449cm^{-1} , 3246cm^{-1} and 3206cm$^{-1,}$ which means respectively the O-H bond for the protonated at the site of the carbonyl, the N-H bond for the protonated on N1 and N2. In aqueous solution, it has a displacement of absorption bands. For Monuron and its three protonated forms, the results show a shift of absorption bands. Indeed, in the case of the different forms protonated on O, N1 and N2, we get respectively 1818cm^{-1} for C=O, 3463cm^{-1} for N-H, 3264cm^{-1} and 3289cm^{-1} for NH^+, 3549 cm^{-1} for the binding OH^+.

4. CONCLUSION

The theoretical study has been conducted using DFT/6-311++G(d,p). The model chemistry has contributed in verifying the stability of the two conjugate acid forms of Monuron through a comparative energetic based analysis. It has been also demonstrated that protonation does not affect the overall geometry. However, these calculations have shown that the energies of formation of all mono-protonated compounds are very close and concluded that protonation on the nitrogen N1 is the most favorable. Despite of the carbonyl oxygen protonation path, the Frontier orbital analysis has shown that the protonation products present larger energy gap and more stability. The analysis of the chemical reactivity of Monuron in the gas and the aqueous phases, through the global and the local reactivity descriptors IP, EA, μ, η, ω, N, indicates that the electrophilic attack is targeting the most nucleophilic site: N1 nitrogen of the urea. The deviations in vibrational frequencies for the neutral and the protonated forms are used to discuss the experimental results.

5. REFERENCES

[1] Sa, F., D. López Malo, and J. Martínez Calatayud, *Determination of the Herbicide Fluometuron by Photo-induced Chemiluminescence in a Continuous-flow Multicommutation Assembly.* Analytical letters. 2007, 40 (15): 2872-2885.

[2] Witkowski, P.T., et al., *Phylogenetic analysis of a newfound bat-borne hantavirus supports a laurasiatherian host association for ancestral mammalian hantaviruses.* Infection, Genetics and Evolution. 2016, 41 113-119. https://doi.org/10.1016/j.meegid.2016.03.036

[3] Kin, C.M. and T.G. Huat, *Simultaneous Determination of Nine Commercial Pesticide Formulations by Gas Chromatography Multi-Pesticide with an Internal Standard Method.* MALAYSIAN JOURNAL OF CHEMISTRY (MJChem). 2011, 13 (1): 57-62.

[4] Ihlaseh, S.M., et al., *Transcriptional Profile of Diuron-Induced Toxicity on the Urinary Bladder of Male Wistar Rats to Inform Mode of Action.* Toxicological Sciences. 2011, 122 (2): 330-338. 10.1093/toxsci/kfr108

[5] Yin, X.L., et al., *Toxic reactivity of wheat (Triticum aestivum) plants to herbicide isoproturon.* Journal of agricultural and food chemistry. 2008, 56 (12): 4825-4831.

[6] Wolf, A., et al., *Occurrence and distribution of organic trace substances in waters from the Three Gorges Reservoir, China.* Environmental Science and Pollution Research. 2013, 20 (10): 7124-7139.

[7] Četkauskaité, A., U. Grigonis, and J. Beržinskiené, *Biodegradation: selection of suitable model.* Ecotoxicology and environmental safety. 1998, 40 (1-2): 19-28.

[8] Upchurch, R.P. and W. Pierce, *The leaching of monuron from Lakeland sand soil. Part II. The effect of soil temperature, organic matter, soil moisture, and amount of herbicide.* Weeds. 1958, 6 (1): 24-33.

[9] Tanaka, F.S., R.G. Wien, and B.L. Hoffer, *Investigation of the mechanism and pathway of biphenyl formation in the photolysis of monuron.* Journal of Agricultural and Food Chemistry. 1982, 30 (5): 957-963.

[10] Booij, P., et al., *Toxic pressure of herbicides on microalgae in Dutch estuarine and coastal waters.* Journal of Sea Research. 2015, 102 48-56. https://doi.org/10.1016/j.seares.2015.05.001

[11] Hussain, S., et al., *Abiotic and biotic processes governing the fate of phenylurea herbicides in soils: a review.* Critical Reviews in Environmental Science and Technology. 2015, 45 (18): 1947-1998.

[12] Chu, W., et al., *Removal of phenylurea herbicide monuron via riboflavin-mediated photosensitization.* Chemosphere. 2007, 69 (2): 177-183.

[13] Chu, W., et al., *Removal of phenylurea herbicide monuron via riboflavin-mediated photosensitization.* Chemosphere. 2007, 69 (2): 177-183. https://doi.org/10.1016/j.chemosphere.2007.04.055

[14] *Monuron*.

[15] Mulliken, R.S., *A new electroaffinity scale; together with data on valence states and on valence ionization potentials and electron affinities.* The Journal of Chemical Physics. 1934, 2 (11): 782-793.

[16] Cook, M. and M. Karplus, *Electron correlation and density-functional methods.* Journal of Physical Chemistry. 1987, 91 (1): 31-37.

[17] Miranda-Quintana, R.A., *Density functional theory for chemical reactivity.* Conceptual density functional theory and its applications in the chemical domain. Apple Academic Press, Hamilton. 2018.

[18] Levandowski, B.J., et al., *Role of orbital interactions and activation strain (distortion energies) on Reactivities in the normal and inverse electron-demand cycloadditions of strained and unstrained cycloalkenes.* The Journal of organic chemistry. 2017, 82 (16): 8668-8675.

[19] Ciraci, S., *A study on the tight-binding method.* Journal of Physics and Chemistry of Solids. 1975, 36 (6): 557-561. https://doi.org/10.1016/0022-3697(75)90141-9

[20] Geldart, D. and M. Rasolt, *Exchange and correlation energy of an inhomogeneous electron gas at metallic densities.* Physical Review B. 1976, 13 (4): 1477.

[21] Becke, A.D., *Density-functional thermochemistry. V. Systematic optimization of exchange-correlation functionals.* The Journal of chemical physics. 1997, 107 (20): 8554-8560.

[22] Boese, A.D., *Assessment of coupled cluster theory and more approximate methods for hydrogen bonded systems.* Journal of chemical theory and computation. 2013, 9 (10): 4403-4413.

[23] Frisch, M.J., et al., *Gaussian 16 Rev. C.01*. 2016: Wallingford, CT.

[24] Van Leeuwen, R. and E. Baerends, *Exchange-correlation potential with correct asymptotic behavior.* Physical Review A. 1994, 49 (4): 2421.

[25] Stewart, J.J., *Optimization of parameters for semiempirical methods II. Applications.* Journal of computational chemistry. 1989, 10 (2): 221-264.

[26] Cammi, R., *Quantum cluster theory for the polarizable continuum model. I. The CCSD level with analytical first and second derivatives.* The Journal of chemical physics. 2009, 131 (16): 164104.

[27] Fedorov, D.G., et al., *The polarizable continuum model (PCM) interfaced with the fragment molecular orbital method (FMO).* Journal of computational chemistry. 2006, 27 (8): 976-985.

[28] Khadrani, A., et al., *Degradation of three phenylurea herbicides (chlortoluron, isoproturon and diuron) by micromycetes isolated from soil.* Chemosphere. 1999, 38 (13): 3041-3050.

[29] Dupuy, N., et al., *Characterization of aqueous and solid inclusion complexes of diuron and isoproturon with β-cyclodextrin.* Applied spectroscopy. 2004, 58 (6): 711-718.

[30] Mendoza-Huizar, L.H., *Global and local reactivity descriptors for picloram herbicide: a theoretical quantum study.* Química Nova. 2015, 38 (1): 71-76.

[31] Gražulis, S., et al., *Computing stoichiometric molecular composition from crystal structures.* Journal of applied crystallography. 2015, 48 (1): 85-91.

[32] Gražulis, S., et al., *Crystallography Open Database–an open-access collection of crystal structures.* Journal of applied crystallography. 2009, 42 (4): 726-729.

[33] Gražulis, S., et al., *Crystallography Open Database (COD): an open-access collection of crystal structures and platform for world-wide collaboration.* Nucleic acids research. 2012, 40 (D1): D420-D427.

[34] Quirós, M., et al., *Using SMILES strings for the description of chemical connectivity in the Crystallography Open Database.* Journal of cheminformatics. 2018, 10 (1): 1-17.

[35] Merkys, A., et al., *COD:: CIF:: Parser: an error-correcting CIF parser for the Perl language.* Journal of applied crystallography. 2016, 49 (1): 292-301.

[36] Downs, R.T. and M. Hall-Wallace, *The American Mineralogist crystal structure database.* American Mineralogist. 2003, 88 (1): 247-250.

[37] Mendoza-Huizar, L.H., *Chemical reactivity of isoproturon, diuron, linuron, and chlorotoluron herbicides in aqueous phase: A theoretical quantum study employing global and local reactivity descriptors.* Journal of Chemistry. 2015, 2015.

[38] Gázquez, J.L., *Perspectives on the density functional theory of chemical reactivity.* Journal of the Mexican Chemical Society. 2008, 52 (1): 3-10.

[39] Liu, S.-B., *Conceptual density functional theory and some recent developments.* Acta Physico-Chimica Sinica. 2009, 25 (3): 590-600.

[40] Ayers, P.W. and M. Levy, *Perspective on "Density functional approach to the frontier-electron theory of chemical reactivity"*. Theoretical Chemistry Accounts. 2000, 103 (3-4): 353-360.

[41] Chermette, H., *Chemical reactivity indexes in density functional theory.* Journal of Computational Chemistry. 1999, 20 (1): 129-154.

[42] Parr, R.G., L.v. Szentpaly, and S. Liu, *Electrophilicity index.* Journal of the American Chemical Society. 1999, 121 (9): 1922-1924.

[43] Parr, R.G., *Density functional theory of atoms and molecules*, in *Horizons of Quantum Chemistry*. 1980, Springer. p. 5-15.

[44] Ayers, P.W. and R.G. Parr, *Variational principles for describing chemical reactions: the Fukui function and chemical hardness revisited.* Journal of the American Chemical Society. 2000, 122 (9): 2010-2018.

[45] Otero, N., et al., *Establishing the pivotal role of local aromaticity in the electronic properties of boron-nitride graphene lateral hybrids.* Physical Chemistry Chemical Physics. 2016, 18 (36): 25315-25328.

[46] Yang, W. and R.G. Parr, *Hardness, softness, and the fukui function in the electronic theory of metals and catalysis.* Proceedings of the National Academy of Sciences. 1985, 82 (20): 6723-6726.

[47] Tazi, R., et al., *Theoretical Approach of the Adsorption of Herbicide Amitrole on the Soil using DFT Method.* Oriental Journal of Chemistry. 2018, 34 (3): 1240-1248.

[48] Gunasekaran, S., et al., *Vibrational spectra and molecular structural investigation of quiniodochlor*. 2004.

How to cite this article:
Masmoudi R, Khettaf S, Boukhatem I, Aberkane R, Kahlat C, Soltani A, Dibi A.Theoretical study of the reactivity of monuron and its protonated forms. J. Fundam. Appl. Sci., 2020, *12(2), 538-562.*